

The Redox Chemistry of the Covalently Immobilized Native and Low-pH Forms of Yeast Iso-1-cytochrome *c*

Carlo Augusto Bortolotti,^{†,‡} Gianantonio Battistuzzi,[†] Marco Borsari,[†] Paolo Facci,[‡] Antonio Ranieri,[†] and Marco Sola^{*,†,‡}

Contribution from the Department of Chemistry and SCS Center, University of Modena and Reggio Emilia, Via Campi 183, I-41100 Modena, Italy, and CNR-INFM National Center nanoStructures and bioSystems at Surfaces-S3, Via Campi 213/A, I-41100 Modena, Italy

Received November 8, 2005; E-mail: sola.marco@unimore.it

Abstract: Cyclic voltammetry experiments were carried out on native *Saccharomyces cerevisiae* iso-1-cytochrome *c* and its C102T/N62C variant immobilized on bare polycrystalline gold electrode through the S–Au bond formed by a surface cysteine. Experiments were carried out at different temperatures (5–65 °C) and pH values (1.5–7). The $E^{\circ'}$ value at pH 7 (+370 mV vs SHE) is approximately 100 mV higher than that for the protein in solution. This difference is enthalpic in origin and is proposed to be the result of the electrostatic repulsion among the densely packed molecules onto the electrode surface. Two additional electrochemical waves are observed upon lowering the pH below 5 ($E^{\circ'} = +182$ mV) and 3 ($E^{\circ'} = +71$ mV), which are attributed to two conformers (referred to as “intermediate” and “acidic”, respectively) featuring an altered heme axial ligation. This is the first determination of the reduction potential for low-pH conformers of cytochrome *c* in the absence of denaturants. Since the native form of cytochrome *c* can be restored, bringing back the pH to neutrality, the possibility offered by this transition to reversibly modulate the redox potential of cytochrome *c* is appealing for bioelectronic applications. The immobilized C102T/N62C variant, which differs from the native protein in the orientation of the heme group with respect to the electrode, shows very similar reduction thermodynamics. For both species, the rate constant for electron transfer between the heme and the electrode increases for the acidic conformer, which is also found to act as a biocatalytic interface for dioxygen reduction.

Introduction

Electron-transfer proteins and redox enzymes should be immobilized on either bare or modified electrode surfaces in order to be used as active constituents in chemical sensors and other biomolecular electronic devices.^{1–3} The stable binding of redox proteins to electrode surfaces with retention of electron transfer (ET) activity has been reported for several protein-electrode combinations.^{4,5} For example, this is the case of cytochromes adsorbed on ITO⁶ and modified metal electrodes,^{7–9} blue copper proteins immobilized on both bare and functionalized surfaces,^{10,11} and cytochrome P450 bound to SAMs.¹²

Even though many binding approaches have been developed, the stability of these protein (sub)monolayers toward temperature and pH is still poorly characterized. However, verifying the retention of electron transfer efficiency at extreme values of temperature and pH may be very important to establish whether an adsorbed protein can be successfully used as a component of electronic biodevices.

Iso-1-cytochrome *c* from *Saccharomyces cerevisiae* (YCC) is generally considered to be a suitable candidate for bioelectronic applications since it contains a single surface cysteine residue (Cys102) that can be exploited for specific tethering, ensuring unique orientation of the protein.^{13,14} Such a feature becomes particularly important for the design of protein–electrode interfaces, since it has been demonstrated that the current flowing through bioelectronic devices can be considerably larger if the conductive molecular carpet is made of uniformly rather than randomly oriented proteins.¹ Recently, YCC has been covalently bound on bare gold surfaces via

[†] University of Modena and Reggio Emilia.

[‡] CNR-INFM National Center-S3.

- (1) Rinaldi, R.; Biasco, A.; Cingolani, G.; Cingolani, R.; Alliata, D.; Andolfi, L.; Facci, P.; De Rienzo, F.; Di Felice, R.; Molinari, E.; Verbeet, M.; Canters, G. *Appl. Phys. Lett.* **2003**, *82*, 472–474.
- (2) Rinaldi, R.; Biasco, A.; Maruccio, G.; Cingolani, R.; Alliata, D.; Andolfi, L.; Facci, P.; De Rienzo, F.; Di Felice, R.; Molinari, E. *Adv. Mater.* **2002**, *14*, 1453–1457.
- (3) Birge, R. R. *Molecular and Biomolecular Electronics*; Oxford University Press: New York, 1994.
- (4) Armstrong, F. A.; Wilson, G. S. *Electrochim. Acta* **2000**, *45*, 2623–2645.
- (5) Fedurco, M. *Coord. Chem. Rev.* **2000**, *209*, 263–331.
- (6) El Kasmi, A.; Leopold, M. C.; Galligan, R.; Robertson, R. T.; Saavedra, S. S.; El Racemi, K.; Bowden, E. F. *Electrochem. Commun.* **2002**, *4*, 177–181.
- (7) Murgida, D. H.; Hildebrandt, P. *J. Phys. Chem. B* **2001**, *105*, 1578–1586.
- (8) Nahir, T. M.; Bowden, E. F. *J. Electroanal. Chem.* **1996**, *410*, 9–13.
- (9) Gavioli, G.; Borsari, M.; Cannio, M.; Ranieri, A.; Volponi, G. *J. Electroanal. Chem.* **2004**, *564*, 45–52.

- (10) Fristrup, P.; Grubb, M.; Zhang, J.; Christensen, H. E. M.; Hansen, A. M.; Ulstrup, J. *J. Electroanal. Chem.* **2001**, *511*, 128–133.
- (11) Chi, Q. J.; Zhang, J. D.; Andersen, J. E. T.; Ulstrup, J. *J. Phys. Chem. B* **2001**, *105*, 4669–4679.
- (12) Fantuzzi, A.; Fairhead, M.; Gilardi, G. *J. Am. Chem. Soc.* **2004**, *126*, 5040–5041.
- (13) Stayton, P. S.; Olinger, J. M.; Jiang, M.; Bohn, P. W.; Sligar, S. G. *J. Am. Chem. Soc.* **1992**, *114*, 9298–9299.
- (14) Gerunda, M.; Bortolotti, C. A.; Alessandrini, A.; Sola, M.; Battistuzzi, G.; Facci, P. *Langmuir* **2004**, *20*, 8812–8816.

Cys102, obtaining a fast and reversible electron transfer with retention of protein functionality.¹⁵ Here, we have studied the redox behavior of native and mutated cytochrome *c* vectorially immobilized on unmodified gold electrodes at varying temperatures and pH values.

Variable temperature direct electrochemistry experiments are informative on protein thermal stability but also allow the reduction potential (E°) to be partitioned into its enthalpic and entropic contributions.^{16,17} This approach helps understanding how surface interactions affect the bonding features and the electrostatics at the prosthetic metal center and the conformational and solvation properties in the two redox states of the protein, which are the ultimate determinants of E° in metallo-proteins.¹⁸ Chemisorption of YCC onto an electrode surface also allows insights to be gained into the acid–base equilibria affecting the redox properties of cytochrome *c* at low pH. It is well-known that cytochrome *c* undergoes conformational transitions as a function of pH in both redox states.¹⁹ The transitions of the ferri form at alkaline pH values were extensively characterized electrochemically.^{20,21} However, much less is known about those occurring in acidic conditions. This is because low pH values induce protonation and detachment from the electrode surface of the SAM of “promoters” used in the direct electrochemistry of freely diffusing cytochrome *c*,^{22–24} thus hampering protein–electrode communication. Diffusionless electrochemistry of YCC on bare gold, which does not require electrode functionalization, thus offers a valuable tool for the investigation of the redox behavior of YCC at low pH. In this respect, the results obtained in this work are unprecedented.

Here, we have also investigated the N62C/C102T mutant of YCC (N62C thereafter), which contains a single cysteine in a different position with respect to the native form (Figure 1), with the aim to comprehend how protein orientation toward the electrode affects the properties of the immobilized biomolecule. The low-pH transition(s) and the resulting conformers were found to be interesting candidates as a molecular switch of E° and biocatalytic constituents, respectively, for use in biomolecular electronic and sensing devices.

Experimental Section

Materials. Iso-1-cytochrome *c* from the yeast *S. cerevisiae* was purchased from Sigma. The samples featured an R_z value ($R_z = A_{410}/A_{280}$) greater than 4.5 and were used without further purification.^{20,25,26} The N62C mutant was produced using the QuikChange XL site-directed mutagenesis kit (Stratagene) starting from two synthetic oligonucleotide

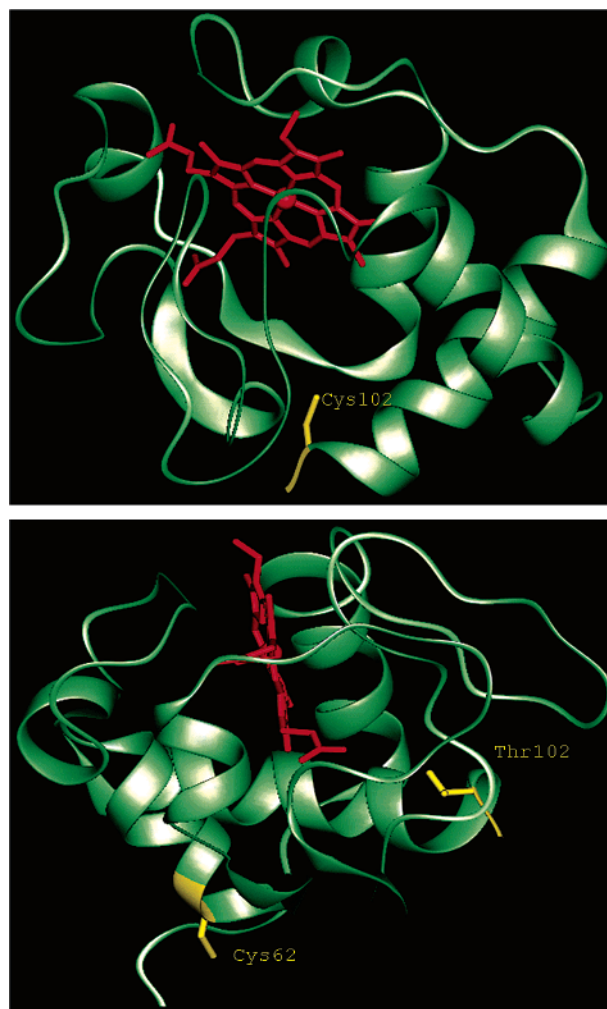


Figure 1. 3D representations of the structures of native (top) and the C102T/N62C mutant (bottom) of *S. cerevisiae* iso-1-cytochrome *c*. Mutations C102T and N62C shown in the figure were produced using the software package QUANTA 2000 (Molecular Simulation Inc, Waltham, MA). Heme is represented in red, and native Cys102 and mutated residues are represented in yellow.

primers carrying the desired mutation and using as DNA template the plasmid pMSV1, which was kindly donated by Prof. M. S. Viezzoli of the University of Florence. This plasmid expresses the C102T variant of yeast iso-1-cytochrome *c* from the pTrc promoter and confers ampicillin resistance. Therefore, the N62C variant carries a cysteine residue in position 62 and a threonine in place of the native Cys102. Protein expression and purification were carried out as described elsewhere.²⁵ All chemicals were reagent grade. Nanopure water was used throughout.

Electrochemistry. Cyclic voltammetry experiments were carried out with a potentiostat/galvanostat PAR model 273A under argon. A polycrystalline gold wire was used as a working electrode and a Pt wire and a saturated calomel electrode (SCE) were used as counter and reference electrode, respectively. The electrical contact between the SCE and the working solution was obtained with a Vycor set. Potentials were calibrated against the MV^{2+}/MV^+ couple²¹ (MV = methyl viologen). All the redox potentials reported here are referred to standard hydrogen electrode (SHE). All the electrochemical measurements involving YCC both adsorbed and in solution were carried out in 0.01 M phosphate buffer in the presence of 0.2 M sodium chloride.

Diffusion-controlled electrochemical measurements were performed after modification of the electrode surface by dipping a previously polished gold electrode into a 1 mM solution of 4-mercaptopyridine for 120 s and then rinsing it with MILLIQ water. Protein solutions

- (15) Heering, H. A.; Wiertz, F. G. M.; Dekker, C.; de Vries, S. *J. Am. Chem. Soc.* **2004**, *126*, 11103–11112.
- (16) Battistuzzi, G.; Borsari, M.; Francia, F.; Sola, M. *Biochemistry* **1997**, *36*, 16247–16258.
- (17) Battistuzzi, G.; Borsari, M.; Loschi, L.; Righi, F.; Sola, M. *J. Am. Chem. Soc.* **1999**, *121*, 501–506.
- (18) Sola, M.; Battistuzzi, G.; Borsari, M. *Chemtracts: Inorg. Chem.* **2005**, *18*, 73–86.
- (19) Moore, G. R.; Pettigrew, G. W. *Cytochromes c: Evolutionary, Structural, and Physicochemical Aspects*; Springer-Verlag: Berlin, 1990.
- (20) Barker, P. D.; Mauk, A. G. *J. Am. Chem. Soc.* **1992**, *114*, 3619–3624.
- (21) Battistuzzi, G.; Borsari, M.; Ranieri, A.; Sola, M. *Arch. Biochem. Biophys.* **2002**, *404*, 227–233.
- (22) Allen, P. M.; Hill, H. A. O.; Walton, N. J. *J. Electroanal. Chem.* **1984**, *178*, 69–86.
- (23) McLendon, G. *Acc. Chem. Res.* **1988**, *21*, 160–167.
- (24) Eddowes, M. J.; Hill, H. A. O. *J. Chem. Soc., Chem. Commun.* **1977**, 771–772.
- (25) Barker, P. D.; Bertini, I.; Del Conte, R.; Ferguson, S. J.; Hajieva, P.; Tomlinson, E.; Turano, P.; Viezzoli, M. S. *Eur. J. Biochem.* **2001**, *268*, 4468–4476.
- (26) Margoliash, E.; Frohwirt, N. *Biochem. J.* **1959**, *71*, 570–571.

(0.1 mM) were freshly prepared before use in 0.01 M phosphate buffer, 0.2 M NaCl, pH 7.0, and their concentration was checked spectrophotometrically.

YCC was adsorbed on bare gold following a slight modification of the procedure described by Heering and co-workers.¹⁵ In particular, protein monolayers were obtained through incubation of the polycrystalline gold wire in a 10^{-4} M solution of reduced cytochrome *c* in 0.01 M phosphate buffer, pH 8.2, for 24 h. To estimate the % surface coverage, the area of the immersed portion of the wire was carefully calculated after each cyclic voltammetry (CV) session by dipping the bare electrode at exactly the same depth into a solution of an electrochemical standard, ferricinium tetrafluoroborate, recording the CV signal for the standard and then applying the Randles–Sevcik relationship. Apparent standard potentials ($E^{\circ'}$) were calculated as $E^{\circ'} = (E_{pa} + E_{pc})/2$.^{16,27} This is appropriate since α is found to be approximately 0.5 and $E^{\circ'}$ is almost independent of the scan rate in the range 20–500 mV s^{-1} .^{28–33} Cyclic voltammograms at variable scan rate were also recorded to determine the electron-transfer rate constant k_s for the adsorbed protein. k_s values were averaged over five measurements and found to be reproducible within 10%, which was taken as the associate error. The peak current ratio $i_{\text{anodic}}/i_{\text{cathodic}}$ for the neutral form is approximately 1 down to pH 4. At lower pH values, the current ratio decreases. For the acid and intermediate forms, the $i_{\text{anodic}}/i_{\text{cathodic}}$ ratio is close to 0.5. Temperature does not affect appreciably the peak current ratios. The nonunit current ratios may be related to the different ET rate constants for the two redox states of immobilized YCC or to a change of the protein or the protein film induced by reduction, which concur to make reoxidation of the reduced form slower. This is supported by the observation that the $i_{\text{anodic}}/i_{\text{cathodic}}$ ratio increases with decreasing scan rate.

Variable temperature experiments were performed with a nonisothermal electrochemical cell.^{34,35} The reference electrode was kept at constant temperature (20 ± 0.1 °C), while the half cell containing the working electrode and the Vycor junction to the reference electrode were kept under thermostatic control with a water bath and its temperature was varied from 5 to 65 °C. With this experimental configuration, the reaction entropy for reduction of the oxidized protein ($\Delta S^{\circ'}_{\text{rc}}$) is given by:^{34,35}

$$\Delta S^{\circ'}_{\text{rc}} = S^{\circ'}_{\text{red}} - S^{\circ'}_{\text{ox}} = nF(dE^{\circ'}/dT) \quad (1)$$

Thus, $\Delta S^{\circ'}_{\text{rc}}$ was determined from the slope of the plot of $E^{\circ'}$ versus temperature, which turns out to be linear under the assumption that $\Delta S^{\circ'}_{\text{rc}}$ is constant over the limited temperature range investigated. With the same assumption, the enthalpy change ($\Delta H^{\circ'}_{\text{rc}}$) was obtained from the Gibbs–Helmholtz equation, namely as the negative slope of the $E^{\circ'}/T$ versus $1/T$ plot. The nonisothermal behavior of the cell was carefully checked by determining the $\Delta H^{\circ'}_{\text{rc}}$ and $\Delta S^{\circ'}_{\text{rc}}$ values of the ferricyanide/ferrocyanide couple.^{34,35} The pH titrations were performed at constant temperature (20 ± 0.1 °C). The pH was changed by adding small amounts of concentrated NaOH or HCl under fast stirring.

The electrocatalytic reduction of O_2 by immobilized YCC at pH 2 was studied by gradually adding air to the O_2 -free solution at normal atmospheric pressure at 20 °C.

All the electrochemical measurements were performed for both native YCC and the N62C mutant. All the experiments were performed at

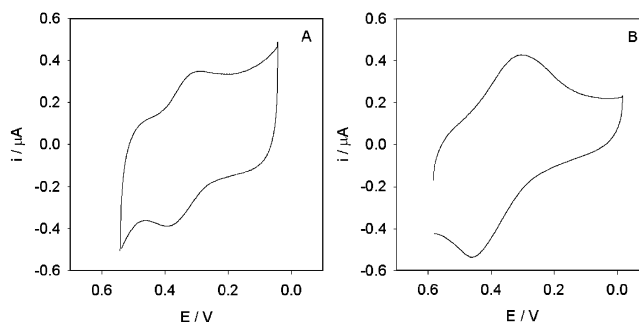


Figure 2. Cyclic voltammograms for native (A) and the C102T/N62C mutant (B) of *S. cerevisiae* iso-1-cytochrome *c* immobilized on bare polycrystalline gold electrode through the (Cys)S–Au bond in 0.01 M phosphate buffer, 0.2 M NaCl, pH 7. Sweep rate, 10 mV s^{-1} . $T = 20$ °C. The different current intensities in A and B are due to differences in the (protein-coated) surface area of the gold electrode put in contact with the working solution in the electrochemical cell.

least five times, and the reduction potentials were found to be reproducible within ± 2 mV.

Results

Electrochemistry of Covalently Immobilized Native Yeast Iso-1-cytochrome *c*. A typical cyclic voltammogram for native YCC immobilized on a bare polycrystalline gold electrode at neutral pH is shown in Figure 2A.

The quasi-reversible cyclic voltammogram originates from the one-electron reduction/oxidation of the YCC in its “neutral” (His, Met-ligated) form. The $E^{\circ'}$ value of +370 mV at pH 7 and 20 °C is 110 mV more positive than that for freely diffusing YCC under identical conditions (+260 mV) (Table 1).

The linear increase of the cathodic peak current with increasing scan rate shows that YCC is immobilized onto the electrode (Figure 3).

This binding does not originate from electrostatic interactions since the electrochemical response is not significantly altered upon addition of 1 M NaCl. Moreover, the absence of any signal for the C102T variant (which does not contain any cysteine) in the same conditions confirms that YCC is covalently bound to the gold via the Au–S(Cys) bond. The rate constant k_s for electron transfer between the heme and the electrode can be estimated from the scan rate dependence of peak potentials using the model proposed by Laviron for diffusionless electrochemical systems (for peak to peak separations greater than 200 mV; see Supporting Information).³⁶ The estimated k_s value for native YCC is $0.20 \pm 0.02 \text{ s}^{-1}$ (Table 2).

The surface coverage of YCC, calculated from the area of the (baseline-corrected) anodic or cathodic peaks, is from 80 to 90% of that expected for a full densely packed monolayer, which would amount to 19 pmol/cm^2 , as estimated from the crystallographic dimensions of the protein.¹⁵

The temperature dependence of $E^{\circ'}$ for immobilized native YCC at pH 7.0 is shown in Figure 4A. The electrochemical response is found to be robust and reversible up to 65 °C. The immobilized protein thus results to be much more stable³⁷ toward temperature than the freely diffusing protein whose CV signal deteriorates above 35 °C.²¹ The $E^{\circ'}$ values show a monotonic linear decrease with increasing temperature from 5

(27) Clark, R. A.; Bowden, E. F. *Langmuir* **1997**, *13*, 559–565.

(28) Willit, J. L.; Bowden, E. F. *J. Phys. Chem.* **1990**, *94*, 8241–8246.

(29) Tarlov, M. J.; Bowden, E. F. *J. Am. Chem. Soc.* **1991**, *113*, 1847–1849.

(30) Song, S. S.; Clark, R. A.; Bowden, E. F.; Tarlov, M. J. *J. Phys. Chem.* **1993**, *97*, 6564–6572.

(31) Ge, B.; Lisdat, F. *Anal. Chim. Acta* **2002**, *454*, 53–64.

(32) Zhang, Z.; Chouchane, S.; Magliozzo R. S.; Rusling, J. F. *Anal. Chem.* **2002**, *74*, 163–170.

(33) Ge, B.; Meyer, T.; Schöning, M. J.; Wollenberger U.; Lisdat, F. *Electrochem. Commun.* **2000**, *2*, 557–561.

(34) Yee, E. L.; Cave, R. J.; Guyer, K. L.; Tyma, P. D.; Weaver, M. J. *J. Am. Chem. Soc.* **1979**, *101*, 1131–1137.

(35) Yee, E. L.; Weaver, M. J. *Inorg. Chem.* **1980**, *19*, 1077–1079.

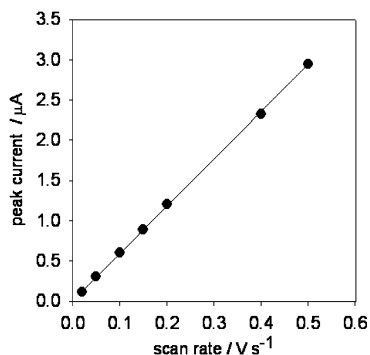
(36) Laviron, E. *J. Electroanal. Chem.* **1979**, *101*, 19–28.

(37) Nicolini, C.; Erokhin V.; Antolini, F.; Catastì, P.; Facci, P. *Biochim. Biophys. Acta* **1993**, *1158*, 273–278.

Table 1. Thermodynamic Parameters for Reduction of *S. cerevisiae* Iso-1-ferricytochrome *c* (YCC) in Solution and Covalently Bound to a Polycrystalline Gold Electrode through a (Cys)S–Au Bond^a

species	$E^{\circ'}$ (mV)		$\Delta H^{\circ'}$ (kJ mol ⁻¹)		$\Delta S^{\circ'}$ (J mol ⁻¹ K ⁻¹)	
	native	N62C	native	N62C	native	N62C
freely diffusing neutral ^d	+260	+263	-37	-38	-44	-45
immobilized neutral ^e	+370	+378	-45	-50	-31	-45
immobilized intermediate ^f	+182	+175	-26	-24	-28	-25
immobilized acidic ^g	+71	+60	-12	-13	-18	-23

^a Average errors on $\Delta H^{\circ'}$ and $\Delta S^{\circ'}$ values are ± 2 kJ mol⁻¹ and ± 6 J mol⁻¹ K⁻¹, respectively. ^b At 20 °C. ^c The sum $(-\Delta H^{\circ'}/F + T\Delta S^{\circ'}/F)$ often does not exactly match $E^{\circ'}$ since the $\Delta H^{\circ'}$ and $\Delta S^{\circ'}$ values are rounded to the closest integer, as a result of experimental error. ^d Phosphate buffer (0.01 M), NaCl (0.2 M), pH 7. “Neutral” conformer stands for the His,Met-ligated heme protein. ^e Phosphate buffer (0.01 M), NaCl (0.2 M), pH 7. ^f At pH 4.5. For “intermediate” conformer, we refer to a species in which probably the heme iron is axially bound by the proximal histidine and a water molecule and experiences a greater exposure to solvent as compared to the neutral conformer (see text). ^g At pH 2. The “acidic” conformer likely features a heme iron with two water molecules as axial ligands and the largest solvent accessibility among the conformers considered here.

**Figure 3.** Scan rate dependence of the cathodic peak current of adsorbed native *S. cerevisiae* iso-1-cytochrome *c* on bare gold. Measurements at variable scan rates were performed in 0.01 M phosphate buffer, 0.2 M NaCl, pH 7, $T = 20$ °C.**Table 2.** Rate Constant for Electron Transfer between the Heme and the Electrode for the Neutral and Acidic Conformers of *S. cerevisiae* Iso-1-ferricytochrome *c* (YCC) and Its N62C Mutant Covalently Bound to a Polycrystalline Gold Electrode through a (Cys)S–Au Bond^a

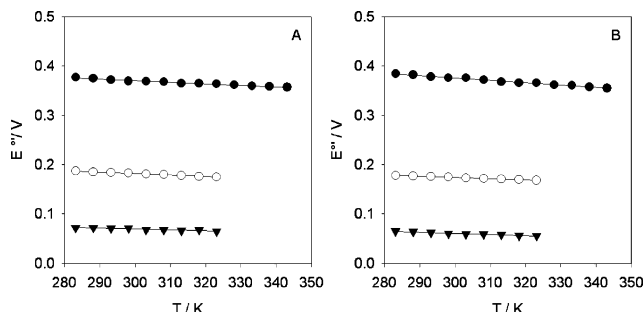
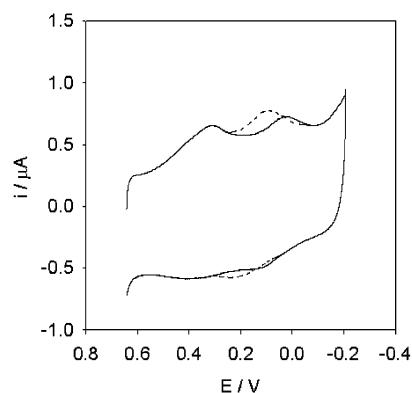
species	k_s (s ⁻¹)	
	native	N62C
neutral conformer ^c	0.20	0.46
acidic conformer ^d	2.2	50

^a Measured from the scan rate dependence of peak potentials using the model proposed by Laviron for diffusionless electrochemical systems.³⁶ ^b At 20 °C; the error affecting the k_s values is $\pm 10\%$. ^c At pH 7. “Neutral” conformer stands for the His,Met-ligated heme protein. ^d At pH 2. The “acidic” conformer likely features a heme iron with two water molecules as axial ligands and the largest solvent accessibility among the conformers considered here.

to 65 °C. The thermodynamic parameters for reduction are listed in Table 1 along with those obtained under diffusion-controlled conditions.

The current intensity of the cathodic peak for immobilized YCC decreases with decreasing pH, and a new wave attributable to an “acidic” conformer appears at more negative potentials ($E^{\circ'} = +71$ mV at pH 2 and 20 °C) and reaches its maximum intensity at pH 1.5 (Figure 5). The conversion of immobilized neutral YCC into the “acidic” form is reversible (namely, an increase in pH back to neutrality leads to the disappearance of the low-potential signal and to the complete recovery of that of the neutral form).

The pH titration of the intensity (measured as the area) of the baseline-corrected cathodic peak for the neutral form is shown in Figure 6A. It is worth noting that, at the lowest pH investigated (1.5), conversion of the immobilized molecules into the acidic form is not complete. At pH values below 1.5, no

**Figure 4.** $E^{\circ'}$ vs T plots for native (A) and the C102T/N62C mutant (B) of *S. cerevisiae* iso-1-cytochrome *c* immobilized on bare polycrystalline gold electrode. (●) Neutral conformer, pH 7.0, $R^2 = 0.985$ (A), $R^2 = 0.989$ (B). (○) “Intermediate” conformer, pH 4, $R^2 = 0.993$ (A), $R^2 = 0.992$ (B). (▼) “Acidic” conformer, pH 2.2, $R^2 = 0.915$ (A), $R^2 = 0.970$ (B). Solid lines are least-square fits to the data points.**Figure 5.** Cyclic voltammograms for native *S. cerevisiae* iso-1-cytochrome *c* immobilized on bare polycrystalline gold electrode through the (Cys102)S–Au bond at pH 2.2 (full line) and pH 4 (dashed line). For sake of clarity, the rest of the voltammogram at pH 4, including the peaks due to the neutral conformer, was erased and only the peaks due to the intermediate conformer were represented. Sweep rate, 20 mV s⁻¹. $T = 20$ °C.

voltammetric signal is detected, probably because of irreversible protein denaturation or formation of an electrochemically silent form. The reduction thermodynamics for immobilized acidic YCC at pH 2 are listed in Table 1. The electron-transfer constant k_s for this conformer (2.2 ± 0.2 s⁻¹) is 1 order of magnitude higher than that for neutral YCC (Table 2). A third electrochemical signal at intermediate potentials ($E^{\circ'} = +182$ at 20 °C) is detected between pH 3 and 5 (Figure 5). The reduction thermodynamics determined for this “intermediate” form of YCC are also listed in Table 1. The pH titrations of the intensity (measured as the area) of the baseline-corrected cathodic peaks for the “acidic” and “intermediate” conformers are shown in Figure 6A.

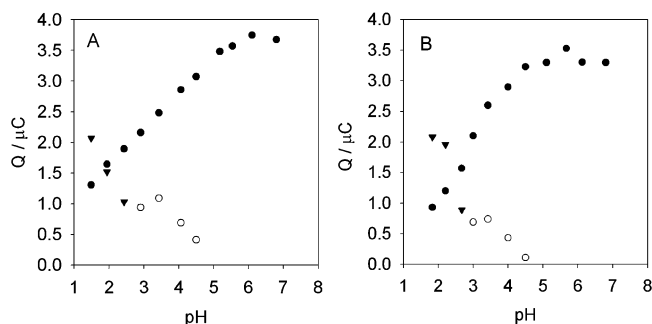


Figure 6. pH dependence of the intensity (measured as the area) of the baseline-corrected cathodic peaks for neutral and low-pH conformers of (A) native and (B) N62C *S. cerevisiae* iso-1-cytochrome *c* immobilized on bare polycrystalline gold electrode through the (Cys)S–Au bond. (●) Neutral (His, Met-ligated) conformer. (○) “Intermediate” conformer. (▼) “Acidic” conformer. $T = 20\text{ }^{\circ}\text{C}$.

Electrochemistry of the Covalently Immobilized N62C Mutant of Yeast Iso-1-cytochrome *c*. Residue 62 was mutated into a cysteine to obtain a covalent immobilization of the protein with a different orientation of the heme toward the gold surface as compared to the native species, yet with a comparable distance between the iron center and the electrode. The edge-to-edge distances between the heme iron atom and the C α carbon of Cys102 and Asn62, calculated from the 3D structure of native yeast cytochrome *c* (PDB code: 1YCC), are 13.9 and 16.1 Å, respectively. Mutation at position 62 was chosen after careful investigation of the three-dimensional structure of native YCC. Asn62 is located at the end of an α helix. Therefore, mutation in this position is likely not to affect the secondary and tertiary structures of the protein. Consistently, the electronic spectra of the mutant coincide with those for native YCC (data not shown). In solution, the N62C variant yields a well-behaved diffusion-controlled electrochemical response as the native form. A typical cyclic voltammogram for chemisorbed N62C on a polycrystalline gold electrode (obtained with the same procedure used for native YCC, which yielded a very similar surface coverage) is shown in Figure 2B. The $E^{\circ'}$ value of +378 mV at pH 7 and 20 °C and the reduction thermodynamics are very similar to those for the native protein. The same holds for the intermediate and acidic forms (Figure 4B and Table 1). Also, the pH titration of the intensity of the cathodic peaks due to the “neutral” His, Met-ligated form and to the low-pH conformers parallels that for native YCC (Figure 6B). The main differences with respect to the native protein involve the ET rate constant k_s , which is approximately two and 20 times larger for the neutral and acid conformer, respectively (Table 2).

Electrocatalytic Reduction of O₂. The sensitivity to oxygen concentration of the acidic form of immobilized native and N62C YCC at pH 2.0 was studied by recording their CV response at increasing O₂ concentration in the electrochemical cell, as previously reported for cytochrome P450.³⁸ An electrocatalytic O₂-reduction wave was observed (Figure 7), which indicated that the acidic YCC layer acts as a biocatalytic interface for dioxygen reduction.

Discussion

Redox Thermodynamics and Kinetics of ET for Immobilized Native YCC. The reduction potential for im-

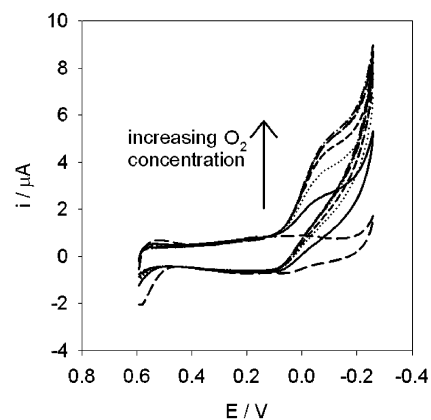


Figure 7. Cyclic voltammograms for the acidic conformer of native *S. cerevisiae* iso-1-cytochrome *c* immobilized on bare polycrystalline gold electrode through the (Cys102)S–Au bond at pH 2 recorded at different exposure times of the electrochemical cell (initially under argon) to air at normal atmospheric pressure. Sweep rate, 20 mV s⁻¹. $T = 20\text{ }^{\circ}\text{C}$.

mobilized native YCC is approximately 100 mV more positive than that for the freely diffusing protein in solution. Such an increase in $E^{\circ'}$ could be a consequence of the strong electrostatic repulsion among the positively charged protein molecules densely packed on the electrode surface, which selectively stabilizes the reduced state (bearing a lower charge). This interpretation is in agreement with the positive shifts in $E^{\circ'}$ reported for cytochrome *c* upon binding to functionalized cationic surfaces (obtained with trimethylammonium-terminated SAMs³⁹) and with the negative $E^{\circ'}$ shifts detected for the binding to anionic surfaces (obtained with COOH-terminated SAMs⁴⁰). These effects are related to the degree of surface coverage, as shown by the decrease in the anodic shift for cytochrome *c* adsorbed on COOH-alkylthiolate SAMs with decreasing surface coverage.²⁷ This may explain the remarkable difference between the present $E^{\circ'}$ value for covalently immobilized YCC ($E^{\circ'} = +0.370\text{ V}$ vs SHE with a coverage of 90% of a full monolayer) and that reported previously ($E^{\circ'} = +0.268\text{ V}$ vs SHE with a coverage of 5–40%).¹⁵

Temperature remarkably influences the redox behavior of both diffusing and adsorbed cytochrome *c*.^{9,16} Our data indicate that surface-immobilized YCC is more thermostable than in solution. This is in line with theoretical predictions⁴¹ and experimental results,⁴² which show that protein adsorption can either alter the population of different conformational states, since spatial confinement may raise the barriers of all dynamic processes in the protein, or shift the equilibrium between different states.

The temperature dependence of $E^{\circ'}$ allows determination of the standard entropy ($\Delta S^{\circ'_{\text{rc}}}$) and enthalpy ($\Delta H^{\circ'_{\text{rc}}}$) changes associated with reduction of the oxidized protein (Table 1). Comparison with the corresponding parameters for the freely diffusing protein shows that the changes in $\Delta H^{\circ'_{\text{rc}}}$ are the main responsible for the $E^{\circ'}$ increase following protein immobilization. This is not unexpected since the enthalpic term also includes the intermolecular electrostatic interactions, which, as noted above, disfavor the oxidized state of immobilized YCC.

(39) Chen, X.; Ferrigno, R.; Yang, J.; Whitesides, G. M. *Langmuir* **2002**, *18*, 7009–7015.

(40) Petrovic, J.; Clark, R. A.; Yue, H.; Waldeck, D. H.; Bowden, E. F. *Langmuir* **2005**, *21*, 6308–6316.

(41) Zhou, H. X.; Dill, K. A. *Biochemistry* **2001**, *40*, 11289–11293.

(42) Cheng, Y. Y.; Chang, H. C.; Hoops, G.; Su, M. C. *J. Am. Chem. Soc.* **2004**, *126*, 10828–10829.

(38) Fleming, B. D.; Tian, Y.; Bell, S. G.; Wong, L. L.; Urlacher, V.; Hill, H. A. O. *Eur. J. Biochem.* **2003**, *270*, 4082–4088.

Changes in intramolecular heme/protein interactions cannot be excluded, although they are likely to play a more limited role. These data thus suggest that YCC immobilization does not alter sensibly the heme moiety and its protein environment.

The modest change in ΔS°_{rc} may reflect immobilization-induced changes in the reorganization of the hydrogen bonding among the water molecules within the hydration sphere of the protein upon reduction, which is the main determinant of the reduction entropy in cytochrome *c* and in ET metalloproteins in general.^{43–48}

The electron-transfer rate between the chemisorbed native YCC and the gold electrode at neutral pH ($0.20 \pm 0.02 \text{ s}^{-1}$) is lower than that found for cytochrome *c* adsorbed on most SAMs (in particular, up to 3 orders of magnitude lower than that for COOH-alkylthiolate SAMs on gold).^{31,49,50} This indicates that covalent immobilization of the protein through the (Cys102)S–Au bond orientation is not competent for fast ET. However, as noted elsewhere,¹⁵ this protein orientation allows interaction of the heme group with redox partners in solution. Moreover, some ET reactions involving adsorbed proteins were found to be rate-limited by conformational reorganization or reorientation at the electrode surface.⁵¹ Therefore, the lateral confinement imposed by the almost full monolayer density of molecules on the electrode could probably affect the electron-transfer rate.

The Low-pH YCC Conformers. The behavior of oxidized cytochrome *c* in solution as a function of pH has been extensively investigated.^{19,52,53} At least four pH-induced conformational transitions have been detected through spectroscopic and electrochemical techniques.^{19,53,54} However, relatively little is known on the pH-dependent equilibria for electrode-immobilized protein films. Covalent S(Cys)–Au binding ensures stable immobilization of YCC onto the electrode surface, which allows electrochemical investigations to be carried out even at very acidic pH values.

Electronic absorption spectroscopy performed on ferricytochrome *c* in solution suggests that a pH decrease to 2 causes the detachment of the two strong axial heme iron ligands (His18 and Met80) and their replacement by water molecules.⁵⁵ The observation of a new CV signal at lower potential ($E^{\circ} = +71 \text{ mV}$ vs SHE) that gradually increases in intensity upon decreasing pH to the detriment of that of the neutral form suggests that YCC undergoes acid-induced conformational changes also when covalently bound on a surface. Although

voltammetric experiments do not allow determination of either the spin state or the identity of the axial ligands for the “acidic” conformer, the dramatic change in E° is consistent with the replacement of both the native axial heme ligands (see below). To our knowledge, this is the first determination of the redox potential for a low-pH cytochrome *c* conformer with an altered axial ligation in the absence of denaturants.⁵⁶

Conformational changes occurring at low pH were previously studied by ¹H NMR⁵⁷ and resonance Raman spectroscopy.⁵⁸ Both techniques are extremely sensitive to small changes around the heme that can be hardly detected by other spectroscopic methods. ¹H NMR data indicate conversion of the native low-spin form into a high-spin intermediate form at a pH of about 4.⁵⁷ A further pH decrease to 2.2 leads to the formation of another high-spin species in slow exchange with the pH 4 conformer. Since both low-pH species are high-spin, in both cases at least one of the two protein axial ligands is detached from the iron. It has been proposed that the high-spin form appearing at pH 4 still features the proximal histidine bound to the iron and that the transition to the other high-spin form at lower pH involves its protonation and detachment from the metal.⁵⁷

The present electrochemical experiments, in agreement with the above NMR data, show the formation of an “intermediate” form in the pH range 3–5, usually appearing as a shoulder of the more intense signals of the neutral or acidic forms, which is clearly detectable only when the pH is lowered very gradually. The presence of such an intermediate species suggests that the conversion of the neutral form to the low-potential acidic form occurs through a sequence of acid–base equilibria. The reduction potential for the intermediate form (+182 mV) falls between those for the neutral and acidic forms (+370 and +71 mV, respectively). The E° values of the two low-pH conformers are consistent with the identity of the axial ligands proposed on the basis of the ¹H NMR results.⁵⁷ We note that the intermediate pH conformer, which should possess a five-coordinate heme group lacking the Met ligand, shows a much greater E° value than that of other species featuring an analogous heme configuration, as microperoxidase-11 (MP-11) ($E^{\circ} = -134 \text{ mV}$)⁴⁴ and HRP ($E^{\circ} = -306 \text{ mV}$).⁴⁴ This can be put in relation with several factors: (i) the present species is covalently attached to the electrode, whereas the E° values for MP-11 and HRP refer to freely diffusing species (YCC immobilization, as discussed above, tends to increase E°), (ii) in HRP the proximal His features a pronounced anionic character, which lowers E° , and (iii) in MP-11 the heme is largely exposed to the solvent, reasonably to a larger extent than in this “intermediate” YCC conformer (see below).

The shape of the pH titration curve of the intensity of the cathodic peak of the neutral form confirms that at low pH YCC undergoes a complex proton-mediated redox chemistry that involves more than one proton and a number of conformational states in equilibrium.^{19,59}

- (43) Battistuzzi, G.; D’Onofrio, M.; Borsari, M.; Sola, M.; Macero, A. L.; Moura, J. J. G.; Rodrigues, P. *J. Biol. Inorg. Chem.* **2000**, *5*, 748–760.
 (44) Battistuzzi, G.; Borsari, M.; Cowan, J. A.; Ranieri, A.; Sola, M. *J. Am. Chem. Soc.* **2002**, *124*, 5315–5324.
 (45) Battistuzzi, G.; Bellei, M.; Borsari, M.; Canters, G. W.; de Waal, E.; Jeuken, L. J. C.; Ranieri, A.; Sola, M. *Biochemistry* **2003**, *42*, 9214–9220.
 (46) Battistuzzi, G.; Borsari, M.; Di Rocco, G.; Ranieri, A.; Sola, M. *J. Biol. Inorg. Chem.* **2004**, *9*, 23–26.
 (47) Battistuzzi, G.; Borsari, M.; Ranieri, A.; Sola, M. *J. Biol. Inorg. Chem.* **2004**, *9*, 781–787.
 (48) Battistuzzi, G.; Borsari, M.; Canters, G. W.; Di Rocco, G.; de Waal, E.; Arendsen, Y.; Leonardi, A.; Ranieri, A.; Sola, M. *Biochemistry* **2005**, *44*, 9944–9949.
 (49) Feng, Z. Q.; Imbayashi, S.; Kakiuchi, T.; Niki, K. *J. Electroanal. Chem.* **1995**, *394*, 149–154.
 (50) Avila, A.; Gregory, B. W.; Niki, K.; Cotton, T. M. *J. Phys. Chem. B* **2000**, *104*, 2759–2766.
 (51) Jeuken, L. J. C. *Biochim. Biophys. Acta* **2003**, *1604*, 67–76.
 (52) Theorell, H.; Åkesson, Å. *J. Am. Chem. Soc.* **1941**, *63*, 1812–1818.
 (53) Wilson, M. T.; Greenwood, C. In *Cytochrome c: A Multidisciplinary Approach*; Scott, R. A., Mauk, G. A., Eds.; University Science Books: Sausalito, CA, 1996; pp 611–634.
 (54) Battistuzzi, G.; Borsari, M.; Loschi, L.; Martinelli, A.; Sola, M. *Biochemistry* **1999**, *38*, 7900–7907.
 (55) Babul, J.; Stellwagen, E. *Biochemistry* **1972**, *11*, 1195–1200.

- (56) Fedurco, M.; Augustynski, J.; Indiani, C.; Smulevich, G.; Antalík, M.; Bánó, M.; Sedláček, E.; Glascock, M. C.; Dawson, J. H. *J. Am. Chem. Soc.* **2005**, *127*, 7638–7646.
 (57) Banci, L.; Bertini, I.; Bren, K. L.; Gray, H. B.; Turano, P. *Chem. Biol.* **1995**, *2*, 377–383.
 (58) Lanir, A.; Yu, N. T.; Felton, R. H. *Biochemistry* **1979**, *18*, 1656–1660.
 (59) Fink, A. L.; Calciano, L. J.; Goto, Y.; Kurotsu, T.; Palleros, D. R. *Biochemistry* **1994**, *33*, 12504–12511.

The reduction thermodynamic data help characterize the molecular events occurring at the heme involved in the transition. The $\Delta H'_{rc}$ values increase in this order: neutral < intermediate < acidic conformer. However, the $\Delta H'_{rc}$ values also contain the contribution from the reduction-induced changes in the hydrogen-bonding strength accompanying reorganization of the water molecules within the hydration sphere of the protein. We have recently shown that, because of solvent-based enthalpy–entropy compensation phenomena, the measured E° changes correspond to the enthalpy change due to protein-based effects without the contribution of solvent reorganization effects.^{45–48} The present results are consistent with the hypothesis that the above conformers differ in axial iron coordination. In particular, the replacement of a methionine with a water molecule in the intermediate form and the further displacement of the proximal His by a second water molecule in the acidic species, both accompanied by an increase in solvent accessibility of the heme, are expected to stabilize the oxidized heme, thus resulting in a decrease in E° . The involvement of a transition-induced increase in heme exposure to solvent results from the comparison of the present E° values with those for MP-11 subjected to changes in axial heme ligation.⁴⁴ In particular, in MP-11 and its adducts with exogenous axial ligands, the heme is largely exposed to the solvent (as testified by the much lower E° values of His₁Met-ligated MP-11 with respect to native cytochrome *c*). As a consequence, the increased heme solvation associated with the removal of one axial ligand is likely not to affect electrostatically E° to a large extent. In MP-11, substitution of an axial Met and an imidazole ligand with a water molecule induces changes in E° of -67 and $+55$ mV, respectively, against corresponding E° changes of -188 and -111 mV accompanying the transition from the neutral to the intermediate form and from the intermediate to the acidic form of YCC, respectively. The pronounced decrease in E° for the two transitions of YCC can be considered as indicative of an increase in solvent accessibility of the heme group, which electrostatically stabilizes the oxidized state. This is also supported by the increase in reduction entropy on passing from the neutral to the intermediate and to the acid form (Table 1). In fact, an increase in solvent accessibility of the heme group is expected to enhance the effect of the partial disruption of the ordering of the surrounding water molecules on reduction due to the decreased electrostatic interaction with the prosthetic center, which formally bears a formal charge of $+1$ and 0 in the oxidized and reduced states, respectively.^{44,46,47,60} The larger exposure of the heme to solvent in the intermediate and low-pH conformers could be simply the result of the removal of axial ligands, although a pH-induced opening of the heme crevice to solvent cannot be excluded, as suggested previously for cytochrome *c* in solution.⁵⁵

The incomplete conversion of immobilized neutral YCC into the acidic conformer is probably due to multiple factors. Cheng and co-workers noticed that covalently immobilized cytochrome *c* features a UV–vis pH titration curve broader than that in solution, which was interpreted as the result of an incomplete conversion of the native into the acid conformer.⁴² Possibly, spatial confinement of immobilized cytochrome *c* leads to a stabilization of the protein in its native conformation. The high

surface coverage probably enhances this effect. As noted above, the tight packing of the adsorbed molecules could hinder their conformational freedom and interfere with the proposed increase in molecular volume associated with the extended conformation of the acidic conformer, as not all the molecules have enough room on the surface of the electrode to undergo the transition. Moreover, it is likely that the pK_a of the transition for each protein is strongly affected by protonation of the surrounding molecules as a consequence of the remarkable intermolecular electrostatic repulsions. Therefore, as a consequence of the very high surface coverage, it is conceivable that: (i) not all the molecules show the same pK_a , which would result in a titration curve more flattened than that in solution, and (ii) the electrostatic repulsion for some of the immobilized biomolecules could be so high as to induce very low pK_a values that prevent protonation (i.e., the acid transition) even at the lowest pH value investigated.

The ET rate constant k_s for the acidic form of the adsorbed native YCC (2.2 ± 0.2 s⁻¹) is approximately 1 order of magnitude larger than that for the neutral form. Conceivably, the partial protein unfolding induced by the increased intramolecular repulsive forces due to the larger net positive charge of the molecules at low pH⁵⁵ alters the ET pathways in the protein matrix. This could also affect the heme orientation and distance from the electrode, resulting in a faster electron transfer process. However, the structural details underlying this effect are presently not at hand.

Effects of YCC Immobilization through the Au–S(Cys62) Bond. The E° and the reduction thermodynamics for the chemisorbed neutral N62C variant are similar to those for native YCC (Table 1). Also, the changes in the reduction thermodynamics upon protein immobilization onto the electrode are comparable. However, whereas covalent binding of native YCC slightly alters the reduction-induced solvent reorganization in the region surrounding Cys102 [since $\Delta\Delta S'^{\circ}_{rc}$ ($\Delta S'^{\circ}_{rc}(\text{adsorbed}) - \Delta S'^{\circ}_{rc}(\text{freely diffusing})$) = -12 J K⁻¹ mol⁻¹], binding of the N62C mutant apparently leaves unaffected that involving the protein patch containing Cys62 (since $\Delta\Delta S'^{\circ}_{rc}$ is zero). The 2-fold increase in k_s for N62C (Table 2) indicates that there is a modest but appreciable effect of protein orientation on the electron-transfer process. The rate of the electron transfer between distant centers (10 – 15 Å or even more) is proportional to the square of the electronic coupling between donor and acceptor, H_{DA} , which depends on the properties of intervening protein medium.^{61,62} Beratan, Onuchic, and co-workers^{63–65} developed an empirical model that allows predictions of the electronic coupling matrix element H_{DA} between donor and acceptor taking the structural complexity of the protein matrix into account (the tunneling Pathway model). The structure-dependent Pathway algorithm searches proteins for the combination of steps that maximizes H_{DA} and assigns different decay parameters to bonded, nonbonded, and hydrogen-bonded steps.⁶⁵ By using this approach, the optimum coupling pathway between two redox sites can be determined, and the relative couplings

(61) Karpishin, T. B.; Grinstaff, M. W.; Komar-Panicucci, S.; McLendon, G.; Gray, H. B. *Structure* **1994**, *2*, 415–422.

(62) Gray, H. B.; Winkler, J. R. *Q. Rev. Biophys.* **2003**, *36*, 341–372.

(63) Beratan, D. N.; Betts, J. N.; Onuchic, J. N. *Science* **1991**, *252*, 1285–1288.

(64) Beratan, D. N.; Betts, J. N.; Onuchic, J. N. *J. Phys. Chem.* **1992**, *96*, 2852–2855.

(65) Jones, M. L.; Kurnikov, I. V.; Beratan, D. N. *J. Phys. Chem. A* **2002**, *106*, 2002–2006.

(60) Battistuzzi, G.; Bellei, M.; Borsari, M.; Di Rocco, G.; Ranieri, A.; Sola, M. *J. Biol. Inorg. Chem.* **2005**, *10*, 643–651.

between a single center (for example, metalloporphyrin, Cu atom, or Fe–S cluster) and any other (nonhydrogen) atom in a protein can be estimated.⁶³ The tunneling pathway model has proved to be one of the most useful methods for estimating distant electronic couplings.⁶² The Pathway algorithm was applied to our system to estimate the coupling matrix element H_{DA} between the heme cofactor and residues 102 and 62, respectively.⁶⁶ Preliminary calculations seem to agree with our experimental results, since C α of Asn62 is predicted to be more strongly coupled to the heme than C α of Cys102. Estimated H_{DA} values between heme and the C α carbon of Cys102 and Asn62 are 1.73×10^{-5} and 8.10×10^{-5} , respectively (arbitrary units, see Supporting Information for further details). This could account for faster ET when the protein is linked to the surface through Cys62 instead of Cys102.

The redox behavior of the mutant at different pH values closely parallels that of native YCC (Table 1). The CV signals and the reduction thermodynamics of the intermediate and acidic forms, which originate at similar pH values, compare well to those of corresponding conformers of native YCC. Thus, the mutant most probably undergoes the same changes in axial heme ligation and exposure to solvent at low pH as native YCC. The shape of the pH titration curve for N62C is slightly different from that of the native protein, suggesting that orientation on the electrode surface influences the way in which the protein reacts to the pH change. This could be because some regions of the protein are more affected than others by the acid transition, according to the finding that 2–4 protons are involved in this pH-induced conformational change.¹⁹

The most remarkable effect induced by the mutation is the increase by more than 100-fold in k_s for the acidic conformer with respect to the neutral one (Table 2), which is 10 times larger than the corresponding k_s increase observed for the native form. Apparently, the pH-induced structural changes of the mutant in proximity of the S(Cys62)–Au bond activate particularly favorable intramolecular ET pathway(s). Thus, the increase in ET efficiency at low pH is affected by the orientation of the heme toward the electrode.

Interaction of the Immobilized “Acidic” Cytochrome *c* Conformer with Molecular Oxygen. Immobilized cytochrome *c* is completely inactive as a biocatalyst for O₂ reduction at neutral pH.⁶⁷ The conformational changes occurring at low pH make the axial coordination positions of the heme iron accessible to molecular oxygen, as previously demonstrated in solution.⁶⁸ These changes should render the active center of the protein more similar to that of redox heme enzymes such as catalase or peroxidase and sensitive to oxygen concentration in solution. Cyclic voltammograms recorded at pH 2.0 for immobilized native YCC and its N62C variant at different O₂ pressures are indicative of a catalytic reduction of dioxygen (Figure 7). This result confirms that at least one axial ligand is detached from the heme iron and replaced by a solvent molecule. Thus, pH-induced conformational modifications could possibly lead to the use of immobilized cytochrome *c* as a component of

biosensing devices. The replacement of redox enzymes by modified ET proteins to achieve catalytic reduction of O₂ or other substrates at the electrode could be particularly useful, since in the former systems direct electrical communication between redox centers and the electrodes is usually hindered by the insulating properties of the protein matrix.^{67,69} Using electron transfer proteins as immobilized components of biosensors could help to at least partially overcome this problem, since these proteins feature internal electronic pathways that evolutionarily evolved to allow fast electron exchange between redox partners. Controlled structural alignment on the electrode surface could possibly lead to satisfactory electrical contact between the metalloprotein and electrode. The use of cytochrome *c* as a biocatalyst presents further advantages,⁷⁰ since the covalent binding of the heme prosthetic group to the protein matrix prevents heme detachment in the presence of organic solvents and the protein is also remarkably stable over a wide range of temperature and pH.

Conclusions

The immobilized low-pH conformers of both native and the C102T/N62C variant of yeast iso-1-cytochrome *c* are found to be electroactive and to reversibly convert to the “neutral” His-, Met-ligated form with pH. The pH-induced difference in $E^{\circ'}$ by 300 mV between the two conformers, due to the detachment of both axial ligands for the heme iron at low pH, could make such a pH-induced conformational transition of use as a molecular switch for bioelectronic devices. One limiting factor is represented by the slow rate of electron transfer between the protein and the electrode, which, however, is found to be remarkably affected by protein orientation toward the electrode itself. Protein orientation can be changed acting on the position of the surface cysteine engineered on the protein surface used to tether the protein to the gold electrode. The change in protein orientation affects only slightly the $E^{\circ'}$ value. Moreover, sensitivity of the acidic conformer toward oxygen, which could be extended also to other substrates, leads to appealing applications of cytochrome *c* in biosensing.

Acknowledgment. This work is dedicated to the memory of Prof. Maria Silvia Viezzoli of the University of Florence. This work was supported by the Ministero dell’Università e della Ricerca Scientifica e Tecnologica of Italy (Programmi di Ricerca Scientifica di Rilevante Interesse Nazionale, PRIN 2003), by the COST D21 action of the European Community (WG D21/0011/01), and MIUR-FIRB “NOMADE”. We thank Dr. Francesca De Rienzo for fruitful discussion.

Supporting Information Available: Scan rate dependence of the anodic and cathodic peak potentials for adsorbed native and N62C mutant of *S. cerevisiae* iso-1-cytochrome *c* on bare gold, individual $E^{\circ'}$ vs T plots (Figure 4) with expanded y-axes, and further details on the prediction of electronic coupling matrix element H_{DA} between heme and residues 62 and 102 using the Pathway algorithm. This material is available free of charge via the Internet at <http://pubs.acs.org>.

JA0573662

(66) Kurnikov, I. V. *Harlem*, <http://www.kurnikov.org/>.

(67) Pardo-Yissar, V.; Katz, E.; Willner, I.; Kotlyar, A. B.; Sanders, C.; Lill H. *Faraday Discuss.* **2000**, *116*, 119–134.

(68) Bren, K. L.; Gray, H. B. *J. Am. Chem. Soc.* **1993**, *115*, 10382–10383.

(69) Heller, A. *Acc. Chem. Res.* **1990**, *23*, 128–134.

(70) Vazquez-Duhalt, R. *J. Mol. Catal. B* **1999**, *7*, 241–249.